Experimental and theoretical investigation of crack width calculation methods for RC ties

Reignard Tan[1,*], Kristoffer Eileraas[1], Ola Opkvitne[1], Giedrius Žirgulis[1], Max A.N. Hendriks[1,2], Mette Geiker[1], Dan-Evert Brekke[3], Terje Kanstad[1]

[1]Norwegian University of Science and Technology, Department of Structural Engineering, 7491 Trondheim, Norway
[2]Delft University of Technology, Faculty of Civil Engineering & Geosciences, 2628CN Delft, the Netherlands
[3]Multiconsult ASA, Nedre Skøyen vei 2, 0276 Oslo, Norway

* Corresponding author at: Multiconsult ASA, Postboks 265 Skøyen, 0213 Oslo, Norway
E-mail address: reignard.tan@multiconsult.no
Contact number: +4741561203

Abstract

This paper theoretically and experimentally investigates the semi-empirical formulas recommended by Eurocode 2 (EC2), fib Model Code 2010 (MC2010), and Eurocode 2 with the German National Annex (DIN) for calculating crack widths in reinforced concrete. It is shown that the formulas can be derived from the principles for the idealized behaviour of RC ties. However, instead of explicitly solving the resulting differential equations, the use of simplifications leads to inconsistent formulas. An experimental study was carried out involving the testing of eight RC ties to discover the modelling uncertainty of the formulas. It was found that EC2 substantially overestimated the crack widths for the RC ties. MC2010 and DIN seemed to predict the crack widths better, but gave rather a large number of non-conservative crack width predictions. These experimental results, combined with the theoretical study, suggest that a more consistent calculation model should be formulated by explicitly solving the resulting differential equation.

Keywords: Crack widths, experiments, calculation methods, modelling uncertainty, semi-empirical formulas, RC ties, cover, tension stiffening, large-scale concrete structures.

1 Introduction

There are several methods for calculating crack widths, and a comprehensive summary of them is provided in Borosnyói and Balász [(2005)]. This study focuses on the semi-empirical formulas for calculating crack widths in cases with relatively large bar diameters and covers, recommended by Eurocode 2 (EC2) [(2004)], *fib* Model Code 2010 (MC2010) [(2013)], and Eurocode 2 with the German National Annex (DIN) [(2011)].

This study is a part of an ongoing research project with the overall objective of improving crack width calculation methods for large-scale concrete structures, i.e. for large cross-sections and thick concrete members. New revisions of EC2 and MC2010 are also currently under way, and this study seeks to contribute by enhancing the crack width calculation methods currently recommended by these codes. The main reason for including DIN in this study is that, unlike EC2 and MC2010, it excludes the cover term in calculating crack distance. The significance of the cover term has been the subject of major discussion in the development of the semi-empirical formulas. Some investigators argue that it should be abandoned [Debernardi and Taliano (2016)], while others claim that it should be dominant [Broms (1968), Gergely and Lutz (1968), Beeby (2004)].

The aim of this study is to investigate how well the formulas comply with the behaviour of RC ties, from both a theoretical and an experimental point of view. First, the idealized behaviour of RC ties is discussed, after which the background theory and the main assumptions used when deriving the semi-empirical formulas is revisited. Then, an experimental study of some relatively large RC ties is presented, which are assumed to be representative of the tensile zones of large cross-sections exposed to bending. Finally, the modelling uncertainty and the theoretical background of the semi-empirical formulas is assessed and investigated.

2 The theoretical background for crack width calculations of RC ties

2.1 The idealized behaviour of RC ties

For simplicity, the idealized behaviour of RC ties is discussed in terms of axisymmetry and using the concept of *slip* as in *fib* bulletin No. 10 [(2000)].

2.1.1 General

Fig. 1 depicts an axisymmetric plane in a RC tie exposed to a tensile force in the steel reinforcement bar ends. The steel bar is shown elongated more than the embedding concrete, and the relative displacement between the materials at an arbitrary section over the transfer length, L_{t}, is considered the slip. The slip consists of two contributions: the relative displacement at the interface between concrete and steel, s_{i}, and the elastic shear deformation in the concrete section, s_{s}; see section 1 in Fig. 1. The sum of the two contributions is the total slip, s_{tot}. The slip at the interface between concrete and steel is normally caused by the non-linear behaviour of the bond due to chemical adhesion and the formation of internal and splitting cracks [Goto (1971), Dörr (1978), Jiang et al. (1984), Tammo et al. (2009)]. The slip caused by elastic shear deformation is a consequence of the force applied at the steel bar end being transmitted to the embedding concrete [Ferry-Borges (1966), Beeby (1979)].

The slip can be conceptually visualized by considering the three different sections in Fig. 1. Both contributions to the total slip are present at section 1 ($s_{\mathrm{tot}} = s_{\mathrm{s}} + s_{\mathrm{i}}$). At section 2, however, the contribution to the total slip is solely due to the elastic shear deformation ($s_{\mathrm{tot}} = s_{\mathrm{s}}$). There is no slip at section 3 implying that any deformation in the concrete and steel is fully compatible, i.e. there is no relative displacement between the materials. This section also marks the end of the transfer length, L_{t}.

2.1.2 Analytical static model

Treating every aspect of the non-linear behaviour of bond can be rather complicated in an analytical static model, and simplifications are needed. One possible simplification is conceptually shown in Fig. 2 by assuming that the sections are statically equivalent. Briefly summarized, the simplification involves treating concrete and steel as elastic materials and lumping all the non-linearity to the interface between concrete and steel by applying a proper bond-slip law. Several authors in the literature [Russo and Romano (1992), Balász (1993), *fib* bulletin No. 52 (2009), Debernardi and Taliano (2016)] have acknowledged this analytical static approach.

2.1.3 Equilibrium and compatibility

The equilibrium and the compatibility of an arbitrary section over the transfer length can now be formulated in accordance with the static model in Fig. 2c). This means that the equilibrium relationships for concrete and steel can respectively be obtained as:

$$\int_{A_{\mathrm{c}}} d\sigma_{\mathrm{c}}\, dA_{\mathrm{c}} = \tau(s_{\mathrm{i}})\pi\phi dx \tag{1}$$

and

$$d\sigma_{\mathrm{s}} A_{\mathrm{s}} = -\tau(s_{\mathrm{i}})\pi\phi dx \tag{2}$$

Note that an integral is generally necessary in Eq. (1) since a certain strain distribution in the concrete section is assumed to occur due to the presence of elastic shear deformation. The strain distribution in the steel section is assumed constant. Furthermore, the relative displacement at the interface between concrete and steel in Fig. 2c) leads to the following compatibility equation for the derivative of the slip:

$$s_{\mathrm{i}}{}'(x) = \frac{ds_{\mathrm{i}}}{dx} = \varepsilon_{\mathrm{si}} - \varepsilon_{\mathrm{ci}} \tag{3}$$

2.1.4 The slip

Using Eq. (1), (2) and (3), and assuming that Hooke's law of elasticity applies for concrete and steel, that Poisson's ratio can be neglected, and that the strain distribution over the concrete section does not vary over the transfer length leads to the following second order ordinary differential equation for the slip:

$$\frac{d^2 s_\mathrm{i}}{dx^2} - \chi\tau(s_\mathrm{i}) = 0 \tag{4}$$

where χ is a constant governing the stiffness relationship between the concrete and steel. To solve Eq. (4), the following boundary conditions can be applied in the *crack formation stage* and the *stabilized cracking stage* respectively:

$$s_\mathrm{i}(L_\mathrm{t}) = 0 \tag{5a}$$
$$s_\mathrm{i}'(L_\mathrm{t}) = 0 \tag{5b}$$

and

$$s_\mathrm{i}(L_\mathrm{t}) = 0 \tag{6a}$$
$$s_\mathrm{i}'(L_\mathrm{t}) > 0 \tag{6b}$$

The crack width, crack distance, longitudinal stress, and strain distribution for the materials can now be obtained by explicitly solving Eq. (4), provided that a proper bond-slip law is applied and that a certain strain distribution over the concrete section is assumed beforehand.

2.2 Semi-empirical formulation

The semi-empirical formulas recommended by EC2, MC2010 and DIN for calculating the crack width can be derived by using the same principles as in the idealized behaviour of RC ties previously discussed. However, it will be shown that simplifications are used instead of explicitly solving Eq. (4) to obtain expressions for the crack width, crack distance, longitudinal stress, and strain distribution of the concrete and steel.

2.2.1 The characteristic crack width

By considering the cracked segment of a RC tie in the stabilized cracking stage (see Fig. 3), the following compatibility equation can be easily derived:

$$w_\mathrm{k} = S_\mathrm{r,max}(\varepsilon_\mathrm{sm} - \varepsilon_\mathrm{cm}) = 2L_\mathrm{t,max}(\varepsilon_\mathrm{sm} - \varepsilon_\mathrm{cm}) \tag{7}$$

where w_k is the characteristic crack width, and $(\varepsilon_\mathrm{sm} - \varepsilon_\mathrm{cm})$ is the difference in longitudinal steel and concrete mean strains over the maximum crack distance, $S_\mathrm{r,max}$, which is defined as twice the maximum transfer length, $L_\mathrm{t,max}$.

2.2.2 Transfer length

The transfer length was originally formulated using the so-called *slip theory* and the *no-slip theory* [Beeby (1979)]. In the slip theory, a slip in the interface between concrete and steel is assumed to occur due to bond failure [Saliger (1936)]. This means solving Eq. (1) under the assumption that the bond-slip function is constant (i.e. $\tau(s_\mathrm{i}) = \tau_\mathrm{bms}$), that plane sections remain plane, and that the concrete stresses at the end of the transfer length do not exceed the

mean tensile strength of concrete f_{ctm} in the stabilized cracking stage, which leads to the following equation for the transfer length:

$$L_{\mathrm{t}\tau} = \frac{1}{4}\frac{f_{\mathrm{ctm}}}{\tau_{\mathrm{bms}}}\frac{\phi}{\rho_{\mathrm{s}}} \tag{8}$$

where $\rho_{\mathrm{s}} = A_{\mathrm{s}}/A_{\mathrm{c,ef}}$ is the reinforcement ratio of the RC tie.

In contrast, the no-slip theory assumes that slip does not occur in the interface between the concrete and steel [Base et al. (1966)]. This means that any slip is solely due to the presence of elastic shear deformation in the concrete section, which reduces the concrete surface stresses and implies that plane sections do not remain plane as in section 2 in Fig. 1. However, no mathematical relationships can be derived and a "traditional engineering rule" is applied instead, with the claim that the transfer length is proportional to the size of the cover *c* as in:

$$L_{\mathrm{t}\alpha} = k_{\alpha}c \tag{9}$$

where the constant k_{α} is empirically determined.

In principle, either theory can be used to calculate the transfer length. However, both theories represent the reported behaviour of RC ties in the literature only to a certain extent [Scott and Gill (1987), Yannopoulos (1989), Fantilli et al. (2007), Tammo and Thelandersson (2009), Borosnyói and Snóbli (2010), Berrocal et al. (2016)]. This resulted in the pragmatic merger of the theories to form the following equation for the maximum transfer length at the time it was formulated [Ferry-Borges (1966)]:

$$L_{\mathrm{t,max}} = L_{\mathrm{t}\alpha} + L_{\mathrm{t}\tau} = k_{\alpha}c + \frac{1}{4}\frac{f_{\mathrm{ctm}}}{\tau_{\mathrm{bms}}}\frac{\phi}{\rho_{\mathrm{s}}} \tag{10}$$

It can be shown that EC2 and MC2010 have adopted this combined concept, however, altering the perception of the contribution related to the no-slip theory. This term seems rather related to the fact that the internal cracks become smaller and eventually close as the distance increases from the steel bar in cases of large covers instead of the elastic shear deformations, which normally are considered negligible [Braam (1990)]. DIN, however, has abandoned the cover term and calculates the maximum transfer length according to Eq. (8), though not exceeding $L_{\mathrm{t}\tau} = \frac{1}{4}\frac{\sigma_{\mathrm{s}}\phi}{1.8f_{\mathrm{ctm}}}$ which accounts for the fact that the transfer length varies in the crack formation stage as stated by [Russo and Romano (1992), Balász (1993), Debernardi and Taliano (2016)].

2.2.3 Mean strains

The mean strains can be derived by assuming a certain longitudinal strain distribution for the concrete and steel in the RC tie in Fig. 3a). Assuming that the mean strains for concrete and steel can be expressed by the same integration constant β yields the following mean strain expressions for steel and concrete respectively:

$$\varepsilon_{\mathrm{sm}} = \varepsilon_{\mathrm{s2}} - \beta\Delta\varepsilon_{\mathrm{sr}} \tag{11}$$

and

$$\varepsilon_{\mathrm{cm}} = \beta \varepsilon_{\mathrm{sr1}} \tag{12}$$

Using that $\Delta\varepsilon_{\mathrm{sr}} = \varepsilon_{\mathrm{sr2}} - \varepsilon_{\mathrm{sr1}}$ and subtracting (12) from (11) yields the following expression for the difference in mean strains:

$$\varepsilon_{\mathrm{sm}} - \varepsilon_{\mathrm{cm}} = \varepsilon_{\mathrm{s2}} - \beta \varepsilon_{\mathrm{sr2}} \tag{13}$$

where $\varepsilon_{\mathrm{s2}} = \sigma_{\mathrm{s}}/E_{\mathrm{s}}$ are the steel strains in a crack in the stabilized cracking stage, $\varepsilon_{\mathrm{sr2}} = \sigma_{\mathrm{sr}}/E_{\mathrm{s}}$ are the steel strains right after a crack has formed in the crack formation stage, and $\varepsilon_{\mathrm{sr1}} = f_{\mathrm{ctm}}/E_{\mathrm{c}}$ are the concrete strains across the section at cracking. The steel stresses right after a crack has formed can be expressed as $\sigma_{\mathrm{sr}} = \frac{f_{\mathrm{ctm}}}{\rho_{\mathrm{s}}}(1 + \alpha_{\mathrm{e}}\rho_{\mathrm{s}})$ when considering the behaviour of a RC tie in the crack formation stage, where $\alpha_{\mathrm{e}} = E_{\mathrm{s}}/E_{\mathrm{c}}$. Inserting these relationships in Eq. (13) finally yields the expression for the difference in mean strains in the stabilized cracking stage as:

$$\varepsilon_{\mathrm{sm}} - \varepsilon_{\mathrm{cm}} = \frac{\sigma_{\mathrm{s}} - \beta \frac{f_{\mathrm{ctm}}}{\rho_{\mathrm{s}}}(1 + \alpha_{\mathrm{e}}\rho_{\mathrm{s}})}{E_{\mathrm{s}}} \tag{14}$$

A similar expression can be derived in the crack formation stage by considering the steel strain distribution for this cracking stage in Fig. 3a). The mean steel strains can then be expressed as: $\varepsilon_{\mathrm{sm}} = \varepsilon_{\mathrm{sr2}} - \beta\Delta\varepsilon_{\mathrm{sr}}$. Using the same procedure as above yields the following expression for the difference in mean strains in the crack formation stage:

$$\varepsilon_{\mathrm{sm}} - \varepsilon_{\mathrm{cm}} = \frac{\sigma_{\mathrm{sr}}}{E_{\mathrm{s}}}(1 - \beta) \tag{15}$$

EC2, MC2010 and DIN have all adopted Eq. (14) for the stabilized cracking stage. In the crack formation stage, however, only MC2010 uses Eq. (15), while EC2 and DIN use the following expression instead:

$$\varepsilon_{\mathrm{sm}} - \varepsilon_{\mathrm{cm}} = 0.6\frac{\sigma_{\mathrm{s}}}{E_{\mathrm{s}}} \tag{16}$$

Hence, Eq. (15) and (16) yields the lower boundary for the difference in mean strains.

3 Experimental study

3.1 Geometry, material properties and test set-up

The behaviour of four square cross-sections (400x400 mm), reinforced with eight deformed steel bars, was experimentally investigated. The bar diameter was either 20 mm or 32 mm, while the cover was either 40 mm or 90 mm; see Fig. 4. The RC ties were pulled in tension and had a total length of 3 metres, of which 2 metres were assumed to be representative for the crack pattern due to the anchorage zones at each end. See Fig. 5 for the test set-up.

The concrete quality was B45 MF40, which is a Norwegian concrete typically used for bridges with a water-to-cement ratio of 0.4. The cement type was Norcem Standard FA Cement and conforms to the requirements of CEM II/B-M 42,5R according to NS-EN 197-1:2011 [(2011)]. The specimens were cured under wet conditions to avoid drying shrinkage. Table 1 shows the compressive strength, tensile strength, and Young's modulus after 28 days. The reinforcement quality was B500NC according to NS 3576 [(2005)] with a yield strength of 500 MPa and Young's modulus 200000 MPa. The threaded rods used in the anchorage zone had a steel quality denoted as 8.8, i.e. with a yield limit of 640 MPa and an ultimate strength of 800 MPa.

An additional set of four parallel RC ties were cast, giving a total of eight RC ties to be investigated in the experimental study. Two identical RC ties were loaded to different loading regimes corresponding to either the crack formation or the stabilized cracking stage. The objective was to study the internal crack pattern at the two load levels by injecting epoxy resin in the cracks. These results will be documented in a subsequent paper, while this paper mainly focuses on the surface cracks. The RC ties were named X-ϕ-c, where X represents the loading regime either as the crack formation (F) or stabilized cracking stage (S), ϕ represents the steel bar diameter and c represents the cover; see Table 2 and Fig. 4.

The tensile force from the loading rig was transferred to the RC tie by mounting a 30 mm thick steel plate with welded ribs onto four M36 rods that were embedded in the anchorage zone at each end; see Fig. 5b). The anchorage of the steel rods inside the specimen was strengthened with steel nuts, while stirrups, additional longitudinal reinforcement, and externally prestressed steel frames were mounted to prevent anchorage failure. The load was applied in a deformation-controlled procedure with a velocity of 0.2 – 0.4 mm/min. Strain gauges were utilized to monitor eccentricities caused by the self-weight of the RC ties or geometric deviations before cracking. The strain measurements showed that these effects were small, which was confirmed by the fact that cracks were usually observed to form instantaneously through the whole section.

3.2 Measuring technique using image analysis

The development of surface cracks was documented using a digital single-lens reflex (DSLR) camera with a 50 mm f/2.5 macro lens mounted to a tripod system; see Fig. 6a) and b). Each crack formed was measured section-wise over a length of 40 mm to the level of the reinforcement; see Fig. 6c), d) and e). This is in agreement with the recommendations in MC2010, i.e. that the crack width measured at the elevation of the reinforcement is comparable to the characteristic crack width. Each section measured was afterwards processed and analysed in the open source program Fiji (ImageJ) [(2012)]. The average crack width for each section measured was then obtained by applying a user-supplied subroutine to the program. Only the crack widths along the vertical faces were documented due to the time consuming measuring technique. This resulted in up to six section average crack width measurements for each crack formed; see Fig. 6d).

One of the main advantages of using this imaging technique is that the inhomogeneous propagation of formed cracks could be properly accounted for, e.g. cracks do not form in a straight line and crack widths vary over the concrete surface; see Fig. 6e).

3.3 Statistical analysis for determining crack widths and modelling uncertainty

The crack widths that are of primary interest from the experimental study and that are comparable to the characteristic crack width, w_k, are the 95%-fractile of the crack widths measured, $w_{0.95}$, for each RC tie. To obtain this value, the statistical method of Engen et al. [(2017)] was used to account for the uncertainty related to the limited number of section average crack width measurements for each formed crack. Generally, the mean and the variance of the crack width for a formed crack i with n_i section average crack width measurements can be estimated as:

$$\bar{y}_i = \frac{1}{n_i}\sum_{j=1}^{n_i} y_{i,j} \tag{17}$$

and

$$S_i^2 = \frac{1}{n_i - 1}\sum_{j=1}^{n_i} (y_{i,j} - \bar{y}_i)^2 \tag{18}$$

where $y_{i,j}$ is the jth section average crack width measurement of crack i. See Fig. 6c) and d) for practical examples of the indexing. Furthermore, it can be shown that the mean and the variance of a group with m formed cracks in a RC tie can be respectively estimated as:

$$\bar{y}_{\text{tot}} = \frac{1}{n_{\text{tot}}}\sum_{i=1}^{m} n_i \bar{y}_i \tag{19}$$

and

$$S_{\text{tot}}^2 = \frac{\sum_{i=1}^{m}([n_i - 1]s_i^2)}{n_{\text{tot}} - 1} + \frac{\sum_{i=1}^{m}(n_i \bar{y}_i^2) - n_{\text{tot}}\bar{y}_{\text{tot}}^2}{n_{\text{tot}} - 1} = s_{\text{tot,w}}^2 + s_{\text{tot,b}}^2 \tag{20}$$

where $n_{\text{tot}} = \sum_{i=1}^{m} n_i$ is the total number of section average crack width measurements in a group with m formed cracks in a RC tie. It should be noted that S_{tot}^2 includes both the variation of the crack width within a formed crack, $s_{\text{tot,w}}^2$, and the variation in the crack width between cracks, $s_{\text{tot,b}}^2$, in a RC tie. The standard deviation, S_{tot}, and the coefficient of variation, V_{tot}, for a group with m formed cracks can now be obtained based on the mean, $\bar{y}_{\text{tot}}$, and variance, S_{tot}^2.

Assuming that the crack widths are normally distributed, a future prediction of the 95%-fractile of the crack width in a RC tie can be estimated as:

$$w_{0.95} = \bar{y}_{\text{tot}} - t_{\alpha=95\%,\nu} S_{\text{tot}} \sqrt{\frac{\nu + 2}{\nu + 1}} \tag{21}$$

where $t_{\alpha=95\%,\nu}$ is the 95%-fractile of the t-distribution with $\nu = n_{\text{tot}} - 1$ degrees of freedom. Based on the estimated 95%-fractile of the crack width, $w_{0.95}$, the modelling uncertainty, θ, can now be calculated as:

$$\theta = \frac{w_{0.95}}{w_{\mathrm{k}}} \tag{22}$$

where w_{k} is the characteristic crack width calculated using the semi-empirical formulas recommended in EC2, MC2010 or DIN. The crack width measured, $w_{0.95}$, can be obtained by assuming both a normal and log-normal distribution of the crack widths. The difference is small and, in the following, only the results assuming log-normally distributed crack widths are presented in accordance with [CEB (1985)]. This means that the natural logarithm of the section average crack width measurement is assumed normally distributed, thus replacing $y_{i,j}$ with $\ln y_{i,j}$ in Eq. (17) and (18). The modelling uncertainty is assumed to be log-normally distributed in accordance with the suggestions in the JCSS Probabilistic Model Code [(2001)].

4 Experimental results

4.1 The modelling uncertainty

The ratio, $s^2_{\mathrm{tot,w}}/s^2_{\mathrm{tot}}$, in Table 2 indicates that the contribution of the within-cracks variation to the total variance, S^2_{tot}, is significant and justifies the use of Eq. (17) to (21). The ratio of $s^2_{\mathrm{tot,w}}/s^2_{\mathrm{tot}} = 1$ in the first two loads steps for S-20-40 can be explained by the fact that only one crack was measured. Furthermore, the relatively low ratio, $s^2_{\mathrm{tot,w}}/s^2_{\mathrm{tot}}$, in the last load steps for S-20-90 and S-32-90 can be explained by the observed variation in crack distances for these members.

The characteristic and measured crack widths at the respective load steps for the RC ties are given in Table 3. The mean material properties in Table 1 were used in determining the characteristic crack widths. Furthermore, the characteristic crack widths determined in accordance with EC2 and MC2010 were based on using the integration constant $\beta = 0.6$ since the RC ties could be considered to be subject to short-term loading only, while a factor of $\beta = 0.4$ was used for DIN in accordance with the provisions in this Annex. It was assumed that the effective concrete area was equal to the cross-sectional area, i.e. $A_{\mathrm{c,ef}} = A_{\mathrm{c}}$. This is reasonable since it was observed that the RC ties usually seemed to crack through the whole section. This assumption was tested by pouring water into the cracks in the top face and observing that it leaked through the whole of the bottom face for RC tie S-32-40, which had the smallest crack widths and a low cover.

The modelling uncertainty for the respective formulas is graphically plotted in Fig. 7 and summarized in Table 4, which shows the mean μ_θ, the standard deviation σ_θ, the coefficient of variation V_θ, and the minimum and maximum values for the modelling uncertainty. The number of observations in which the crack widths measured exceed the crack widths calculated is also shown, i.e. $n(\theta_s > 1)$. In total, 16 values for the crack widths measured $w_{0.95}$ were obtained from the experiments (see Table 2), which gives 16 observations for the modelling uncertainty. The median $w_{0.5}$ is also given to elucidate the scatter of the measurements.

The results show that EC2 has the lowest standard deviation and coefficient of variation, implying that the scatter of the modelling uncertainty around the mean is lower than with MC2010 and DIN. However, EC2 consistently predicts crack widths substantially on the conservative side, which is shown by the low mean value and the relatively low maximum value for the modelling uncertainty. In practice, this implies that EC2 consistently predicts crack widths that are on average more than half the size of the largest crack widths measured

(95%-fractile) in the RC ties. Nevertheless, all of the predicted crack widths according to EC2 are on the conservative side.

MC2010 and DIN seem to predict the crack widths better in terms of the mean for the modelling uncertainty. However, the relatively high standard deviation and coefficient of variation for both codes yields a larger scatter around the mean than with EC2. This implies that MC2010 and DIN predict the crack widths more inconsistently than EC2 and do so occasionally on the non-conservative side. In fact, MC2010 predicts five and DIN predicts seven crack widths that are on the non-conservative side, which are relatively large numbers compared to the total observations for the modelling uncertainty. This is particularly pronounced for the RC ties with large bar diameters and covers; see Table 3. It should be mentioned though, that the reported modelling uncertainties are representative for this experimental series and are not intended to serve as a generalization for the performance of the formulas.

4.2 Crack distances

Table 5 shows the maximum calculated crack distance and the maximum measured crack distances for the RC ties in the stabilized cracking stage, which should be comparable according to the discussions in subsection 2.2.2 above. The mean values are also shown. The table shows that EC2 and MC2010 predict the maximum crack distances on the conservative side in all cases, while DIN underestimates the maximum measurements for S-32-40 and S-32-90. The table also elucidates that the maximum crack distances are more influenced by the cover than the bar diameter. The measured values show that the maximum crack distance increases with increasing cover for a constant reinforcement ratio. This seems to comply with the formulas recommended by EC2 and MC2010, which acknowledge the significance of the cover in calculating the maximum crack distance. However, the increase in the maximum crack distance due to the influence of the cover seems to be dramatically overestimated in EC2, which can be seen from the contribution of the no-slip term, $2L_{t\alpha}$, to the maximum crack distance. MC2010 appears to predict the increase better. Nevertheless, DIN actually gives the best overall agreement with the measured maximum crack distances.

5 Discussion

5.1 Semi-empirical formulas in theory

The composed transfer length in Eq. (10) is conceptually visualized in Fig. 8 in accordance to the origin of the formula, which shows that plane sections remain plane and that a slip in the interface between concrete and steel occurs at section 1 as assumed in the slip theory. Compatibility in deformation is restored on the right-hand side of section 2, which also marks the end of the transfer length according to the slip theory. The addition of the transfer length according to the no-slip theory implies a sudden incompatibility in deformation on the left-hand side of section 2, which means that plane sections no longer remain plane due to the presence of elastic shear deformation. Compatibility is restored at section 3, which marks the end of the transfer length according to the no-slip theory as well as the end of the composed transfer length. In other words, the combined concept implies that compatibility and incompatibility in deformation both occur at the same time at section 2, and that compatibility in deformation occurs twice within the same composed transfer length, at sections 2 and 3. Although the cover term in the transfer length formula recommended by EC2 and MC2010

has a different physical meaning than originally formulated, does not change the fact that the current formulation is in conflict with the basic principles of solid mechanics and violates the equilibrium for the concrete section in Eq. (1). Moreover, a merging of the slip and the no-slip theory, two theories based on exactly opposite assumptions, can be considered inconsistent, ambivalent and controversial from a statics point of view.

5.2 Semi-empirical formulas in practice

An important physical factor is how well the semi-empirical formulas according to EC2, MC2010 and DIN capture the cracking behaviour in the crack formation stage and the stabilized cracking stage. This can be monitored by using Eq. (14), (15) and (16) to indicate the cracking state of the RC ties at the current load level and then comparing it to the observed experimental behaviour; see Table 3. This shows that EC2 assumes that the RC ties are in the crack formation stage except for one load step. This applies even to relatively large steel stresses, such as 321 MPa for S-20-40 and 399 MPa for S-20-90 in the last load steps. MC2010 and DIN seem to capture this better than EC2. For MC2010, the better compliance between the predicted and observed behaviour seems to be related to the fact that the difference in mean strains are explicitly derived based on the assumed behaviour of the RC ties in the crack formation stage, as shown in subsection 2.2.3. The better compliance for DIN seems to be related to the fact that the tension stiffening factor $\beta = 0.4$ seems to fit better than $\beta = 0.6$ in the stabilized cracking stage. Recent studies in the literature also support the idea of reducing the tension stiffening factor in the stabilized cracking stage [Debernardi and Taliano (2016), CEOS.fr (2016)].

The experimental study suggests that the maximum crack distance is significantly influenced by the cover, which is supported by another experimental study in the literature [Caldentey et al. (2013)]. More remarkable is the limited influence of the bar diameter, which contradicts the beneficial effect of using large bar diameters in reducing the transfer length according to the slip term in Eq. (10) and as observed in Table 5. Moreover, DIN does not acknowledge that the crack distance increases with increasing cover under the assumption that $A_{\mathrm{c,ef}} = A_{\mathrm{c}}$, which contradicts the observed behaviour of the RC ties in this experimental study. An interesting point, however, is that DIN gives the best overall agreement with the maximum crack distances measured. These contradictory observations, combined with the theoretical study, suggest that the effect of cover and bar diameter should be implemented more consistently than is done in the current semi-empirical formulas.

5.3 Suggestions for improvements

One suggestion for a more consistent calculation model is to solve Eq. (4) explicitly, by applying a proper bond-slip law that takes into account the bond non-linearity in RC ties and by assuming an appropriate strain distribution over the cover in Eq. (1). In this way, the contribution to the total slip can be consistently accounted for at each section of the RC tie without violating the equilibrium, which is an effect the semi-empirical formulas are essentially attempting to model. Moreover, one of the main advantages of explicitly solving Eq. (4) is that it is not necessary to assume a certain longitudinal strain distribution for concrete and steel to obtain the crack widths. Instead, the chosen bond-slip law and the contribution of the embedding concrete will explicitly account for the tension stiffening. The challenge is then

limited to determining the bond-slip law properties and the strain distribution in the concrete, for instance, by conducting physical and numerical studies. Some of the authors in this paper are currently working on such improvements.

It should be mentioned though, that these suggestions lead to more complex crack width calculations that primarily are intended for large-scale concrete structures, i.e. where the use of large covers and bar diameters is typical. The simplifications in the semi-empirical formulas, however, seem adequate in conventional cases.

6 Conclusion

The behaviour of RC ties has been investigated from both an experimental and a theoretical point of view. The aim was to study the applicability of the semi-empirical formulas recommended by EC2, MC2010 and DIN in predicting crack widths for large-scale concrete structures, where large bar diameters and covers typically are used. The theoretical study showed that the semi-empirical formulas could be derived by using the principles of the idealized behaviour of RC ties. However, instead of solving the resulting differential equation explicitly, simplifications are made, resulting in semi-empirical formulas that account for the physical behaviour of RC ties in a rather inconsistent manner that is also in conflict with the basic principles of solid mechanics.

The conducted experimental study showed that EC2 consistently predicted crack widths that were substantially on the conservative side. MC2010 and DIN seemed to predict the crack widths better, but the relatively large standard deviation and coefficient of variation for the modelling uncertainty resulted in a large number of predicted crack widths on the non-conservative side. This was particularly pronounced for large bar diameters and covers. The experimental study also showed that the cover governs the crack distance and thus the crack widths, which is acknowledged by the semi-empirical formulas in EC2 and MC2010, yet DIN actually gave the best agreement with the crack distances measured even though the cover term is abandoned in this code. The reported modelling uncertainties are representative for this experimental series and are not intended to serve as a generalization for the performance of the formulas.

These contradictory observations, combined with the theoretical study, suggest that a more consistent calculation model should be formulated for large-scale concrete structures. It is proposed that the influence of cover and tension stiffening can be addressed more consistently by (i) selecting a proper bond-slip law, (ii) assuming an appropriate strain distribution over the concrete cover, and (iii) explicitly solving the differential equations for the slip.

Notation

A_{c}	concrete area
$A_{\mathrm{c,ef}}$	effective concrete area
A_{s}	steel area
c	cover
dx	infinitesimal increase x-coordinate
E_{c}	concrete Young's modulus
E_{s}	steel Young's modulus

f_{ctm}	mean tensile strength for concrete
j	section in a crack
k_{α}	empirical constant in the no-slip theory
L_{t}	transfer length
$L_{\mathrm{t,max}}$	maximum transfer length
$L_{\mathrm{t}\alpha}$	transfer length according to no-slip theory
$L_{\mathrm{t}\tau}$	transfer length according to slip theory
n_i	number of section average crack width measurements for a crack in a RC tie
n_{tot}	total number of section average crack width measurements for a group of cracks in a RC tie
m	total number of cracks in a RC tie
P	applied force in the RC ties
s_{i}	slip at interface between concrete and steel
s_{s}	slip caused by shear deformations in the concrete section
s_{tot}	total slip in a section over the transfer length
S_i^2	variance of section average crack width measurements for a crack
S_{tot}^2	variance of total section average crack width measurements for a group of cracks in a RC tie
$S_{\mathrm{r,max}}$	maximum crack distance
V_{θ}	coefficient of variation for the modelling uncertainty
$w_{0,95}$	95%-fractile of the measured crack widths
w_{k}	characteristic crack width
$w_{\mathrm{k,DIN}}$	characteristic crack width recommended by DIN
$w_{\mathrm{k,EC2}}$	characteristic crack width recommended by EC2
$w_{\mathrm{k,MC2010}}$	characteristic crack width recommended by MC2010
X	loading regime for RC ties in either crack formation stage or stabilized cracking stage
$y_{i,j}$	average crack width measurement for the jth section in a crack
$\bar{y}_i$	mean of section average crack width measurements for a crack
$\bar{y}_{\mathrm{tot}}$	mean of total section average crack width measurements for a group of cracks in a RC tie
α_{e}	modular ratio
β	tension stiffening factor
$\Delta\varepsilon_{\mathrm{sr}}$	difference in steel strains at a crack and at the end of transfer length in crack formation stage
$\varepsilon_{\mathrm{ci}}$	longitudinal concrete strains at interface
$\varepsilon_{\mathrm{cm}}$	longitudinal mean concrete strains
$\varepsilon_{\mathrm{s2}}$	steel strains at a crack in stabilized cracking stage
$\varepsilon_{\mathrm{sr1}}$	steel strains at the end of the transfer length in crack formation stage
$\varepsilon_{\mathrm{sr2}}$	steel strains in crack in crack formation stage
$\varepsilon_{\mathrm{sm}}$	longitudinal mean steel strains
$\varepsilon_{\mathrm{si}}$	longitudinal steel strains at interface
μ_{θ}	mean value for the modelling uncertainty
σ_{c}	concrete stress

σ_s	steel stress
σ_{sr}	steel stress at a crack in crack formation stage
σ_θ	standard deviation for the modelling uncertainty
ρ_s	reinforcement ratio
τ	bond stress
τ_{bms}	mean bond stress
ϕ	steel bar diameter
χ	stiffness relationship between concrete and steel

Acknowledgements

The work presented in this paper is a part of an ongoing PhD-study funded by the research projects Ferry-free E39 and Durable Advanced Concrete Structures (DaCS).

References

1. Bálasz, G.L.: Cracking Analysis Based on Slip and Bond Stresses. ACI Materials Journal, Vol. 90, No. 4, pp. 340-348, 1993.
2. Base, G.D., Read, J. B., Beeby, A.W., Taylor, H.P.J.: An investigation of the crack control characteristics of various types of bar in reinforced concrete beams. Research Report 18, Part 1, Cement and Concrete Association, London, 1966.
3. Beeby, A.W.: The prediction of crack widths in hardened concrete. The Structural Engineer, Vol. 57A, No.1, pp. 9-17, 1979.
4. Beeby, A.: The influence of the parameter ϕ/ρ_{eff} on crack widths. *Fib* Journal Structural Concrete, Vol. 5, No.2, pp. 71-83, 2004.
5. Berrocal, C., Löfgren, I., Lundgren, K., Görander, N., Halldén, C.: Characterisation of bending cracks in R/FRC using image analysis. Cement and Concrete Research, Vol. 90, pp. 104-116, 2016.
6. Borosnyói, A., Balász, G.L.: Models for flexural cracking in concrete: the state of the art. *fib* Journal Structural Concrete, vol. 6, No. 2, pp. 53-62, 2005.
7. Borosnyói, A., Snóbli, I.: Crack width variation within the concrete cover of reinforced concrete members, Építőanyag – Journal of Silicate Based and Composite Materials, Vol. 62, No. 3, pp. 70-74, 2010.
8. Braam, C.R.: Control of crack width in deep reinforced concrete beams, PhD thesis, TU Delft, 1990.
9. Broms, B.: Theory of the calculation of crack width and crack spacing in reinforced concrete members. Cement och Betong, Vol. 1, pp. 52-64, 1968. [In Swedish]
10. Caldentey, A.P., Peiretti, H.C., Iribarren, J.P., Soto, A.G.: Cracking of RC members revisited: influence of cover, $\phi/\rho_{s,ef}$ and stirrup spacing – an experimental and theoretical study. *fib* Journal Structural Concrete, Vol. 14, No. 1, pp. 69-78, 2013.
11. CEB: CEB Design Manual on Cracking and Deformations. École Polytechnique Fédérale du Lausanne, Switzerland, 1985.
12. CEN: EN 1992-1-1, Eurocode 2: Design of Concrete Structures – Part 1-1: General Rules and Rules for buildings. European Committee for Standardization, Brussels, 2004.

13. CEOS.fr: Control of Cracking in Reinforced Concrete Structures. ISTE Ltd and John Wiley & Sons, Inc, London and Hoboken, 2016.
14. Debernardi, P.G., Taliano, M.: An improvement to Eurocode 2 and *fib* Model Code 2010 methods for calculating crack width in RC structures, *fib* Journal Structural Concrete, Vol. 17, No. 3, pp. 365-376, 2016.
15. DIN: EN-1992-1-1/NA: 2011-01, National Annex – Nationally determined parameters – Eurocode 2: Design of concrete structures – Part 1-1: General rules and rules for buildings, 2011.
16. Dörr, K.: Bond-behaviour of ribbed reinforcement under transversal pressure, Proceedings of IASS Symposium on Nonlinear Behaviour of Reinforced Concrete Spatial Structures, Darmstadt, 1, Edited by G. Mehlhorn, H. Rühle and W. Zerna, Düsseldorf, Germany, 1978.
17. Engen, M., Hendriks, M. A. N., Köhler, J., Øverli, J. A., Åldstedt, E., Mørtsell, E., Sæter, Ø., Vigre, R.: Predictive strength of ready-mixed concrete: exemplified using data from the Norwegian market. Under review, 2017.
18. Fantilli, A.P., Mihashi, H., Vallini, P.: Crack profile in RC, R/FRCC and R/HPFRCC members in tension. Materials and Structures, Vol. 40, pp. 1099-1114, 2007.
19. Ferry-Borges, J.: Cracking and deformability of reinforced concrete beams. IABSE Publications, Vol. 26, pp. 75-95, 1966.
20. *fib*: Bond of reinforcement in concrete – State-of-art report. *fib* bulletin No. 10, Lausanne, Switzerland, 2000.
21. *fib*: Structural Concrete – Textbook on behaviour, design and performance, Second edition, Volume 2. *fib* bulletin No. 52, Lausanne, Switzerland, 2010.
22. *fib*: *fib* Model Code for Concrete Structures 2010, International Federation for Structural Concrete, Ernst & Sohn, Berlin 2013.
23. Gergely, P., Lutz, L. A.: Maximum Crack Width in Reinforced Concrete Flexural Members. Causes, Mechanisms and Control of Cracking in Concrete, SP-20, American Concrete Institute, Farmington Hills, MI, pp. 87-117, 1968.
24. Goto, Y.: Cracks Formed in Concrete around Deformed Tension Bars. ACI Journal, Vol. 68, No. 4, pp. 244-251, 1971.
25. JCSS: Probabilistic Model Code, 12th draft. Joint Committee on Structural Safety; 2001.
26. Jiang, D.H., Shah, S.P., Andonian, A.T.: Study of the Transfer of Tensile Forces by Bond. ACI Journal, Vol. 81, No. 3, pp. 251-259, 1984.
27. NS: 3576-1:2005, Steel for the reinforcement of concrete – Dimensions and properties – Part 1: Ribbed bars B500NA. SN/K 089, 2005. [In Norwegian]
28. NS: EN-197-1:2011, Cement – Part 1: Composition, specifications and conformity criteria for common cements. SN/K 007, 2011.
29. Russo, G., Romano, F.: Cracking Response of RC Members Subjected to Uniaxial Tension. Journal of Structural Engineering, Vol. 118, No. 5, pp. 1172-1190, 1992.
30. Saliger, R.: High-grade steel in reinforced concrete. Proceedings Second Concress of the International Association for Bridge and Structural Engineering. Berlin-Munich, 1936.
31. Schneider, C.A., Rasband, W.S., Eliceiri, K.W.: NIH Image to ImageJ: 25 years of image analysis. Nature methods, Vol. 9, No. 7, pp. 671-675, 2012.
32. Scott. R.H., Gill, P.A.T.: Short-term distributions of strain and bond stress along tension reinforcement. The Structural Engineer, Vol. 65B, No. 2, pp. 39-48, 1987.

33. Tammo, K., Lundgren, K., Thelandersson, S.: Nonlinear analysis of crack widths in reinforced concrete. Magazine of Concrete Research, Vol. 61, No. 1, pp. 23-34, 2009.
34. Tammo, K., Thelandersson, S.: Crack behavior near reinforcing bars in concrete structures. ACI Structural Journal, Vol. 106, No. 3, pp. 259-267, 2009.
35. Yannopoulos, P.J.: Variation of concrete crack widths through the concrete cover to reinforcement. Magazine of Concrete Research, Vol. 41, No. 147, pp. 63-68, 1989.

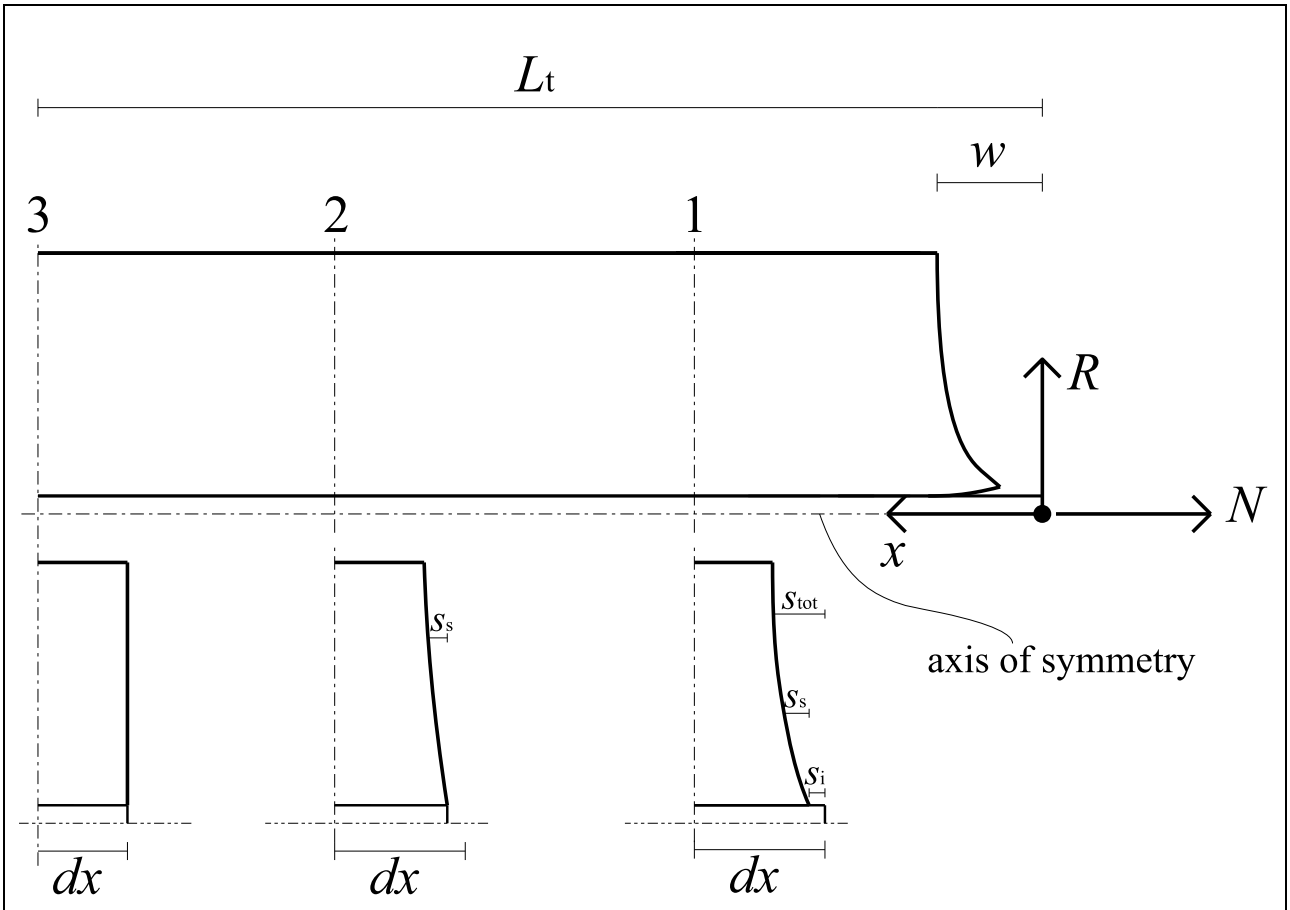

Fig. 1. Idealized behaviour of RC ties and the definition of slip

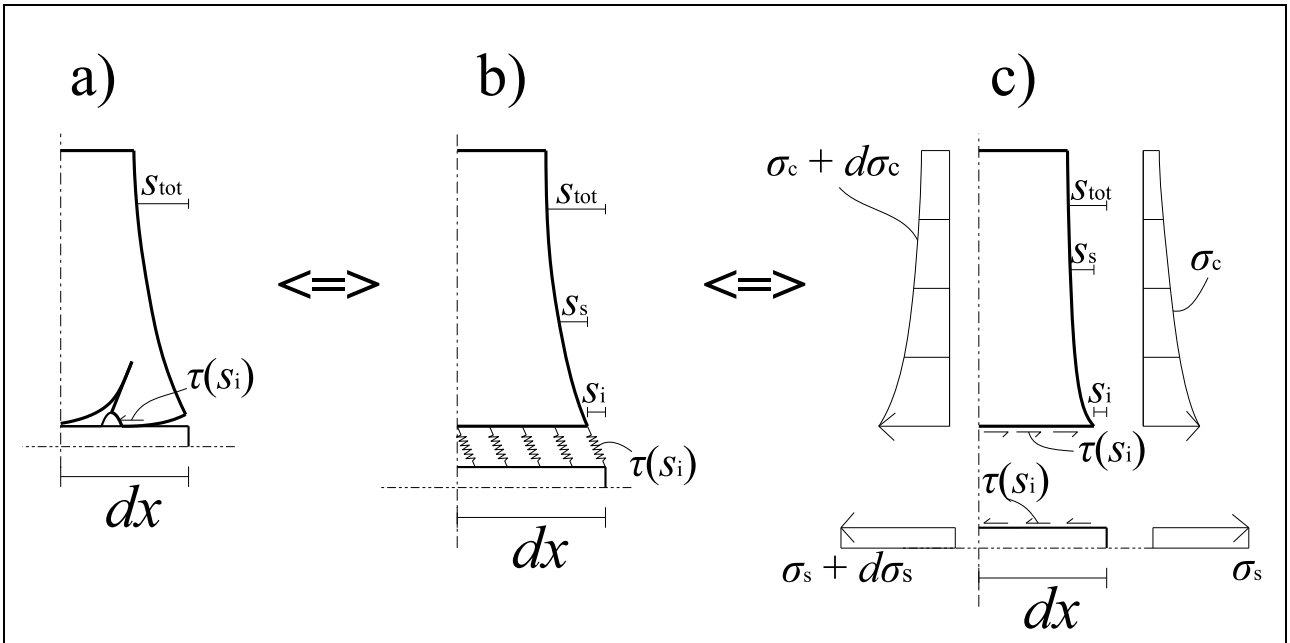

Fig. 2. Statically equivalent sections: a) "True" behaviour of bond non-linearity caused by loss of adhesion and formation of internal and splitting cracks; b) Bond non-linearity lumped as spring behaviour to the interface between concrete and steel; c) Simplified static model assuming that the bond non-linearity in the spring can be modelled with a proper bond-slip law

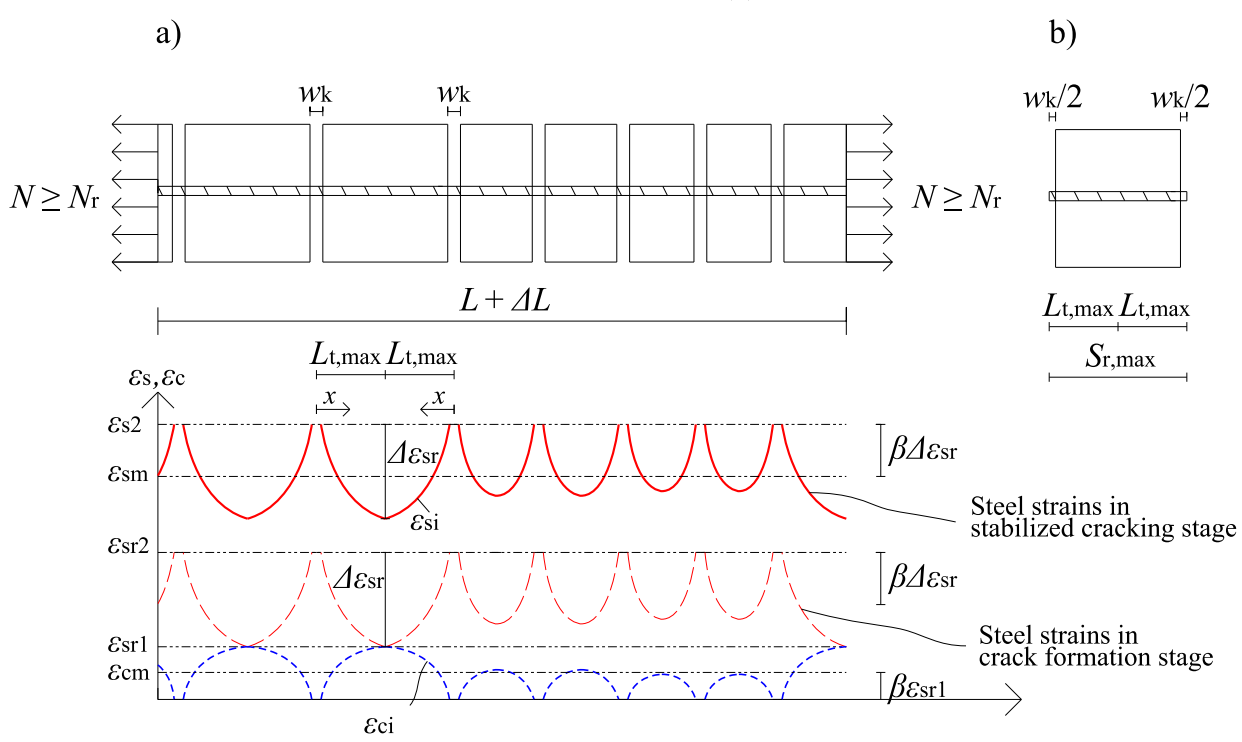

Fig. 3. Cracked RC tie: a) Strain distribution in a fully cracked RC Tie; b) Cracked segment in an RC tie

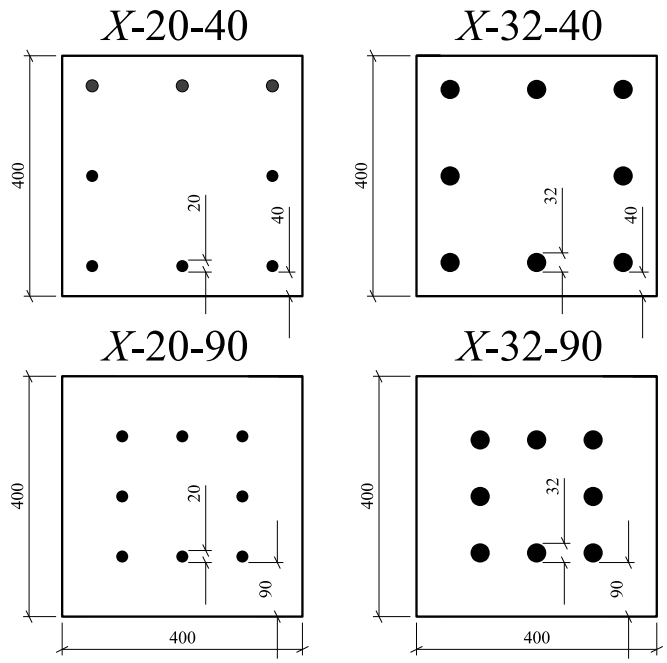

Fig. 4. Cross-sections of RC ties

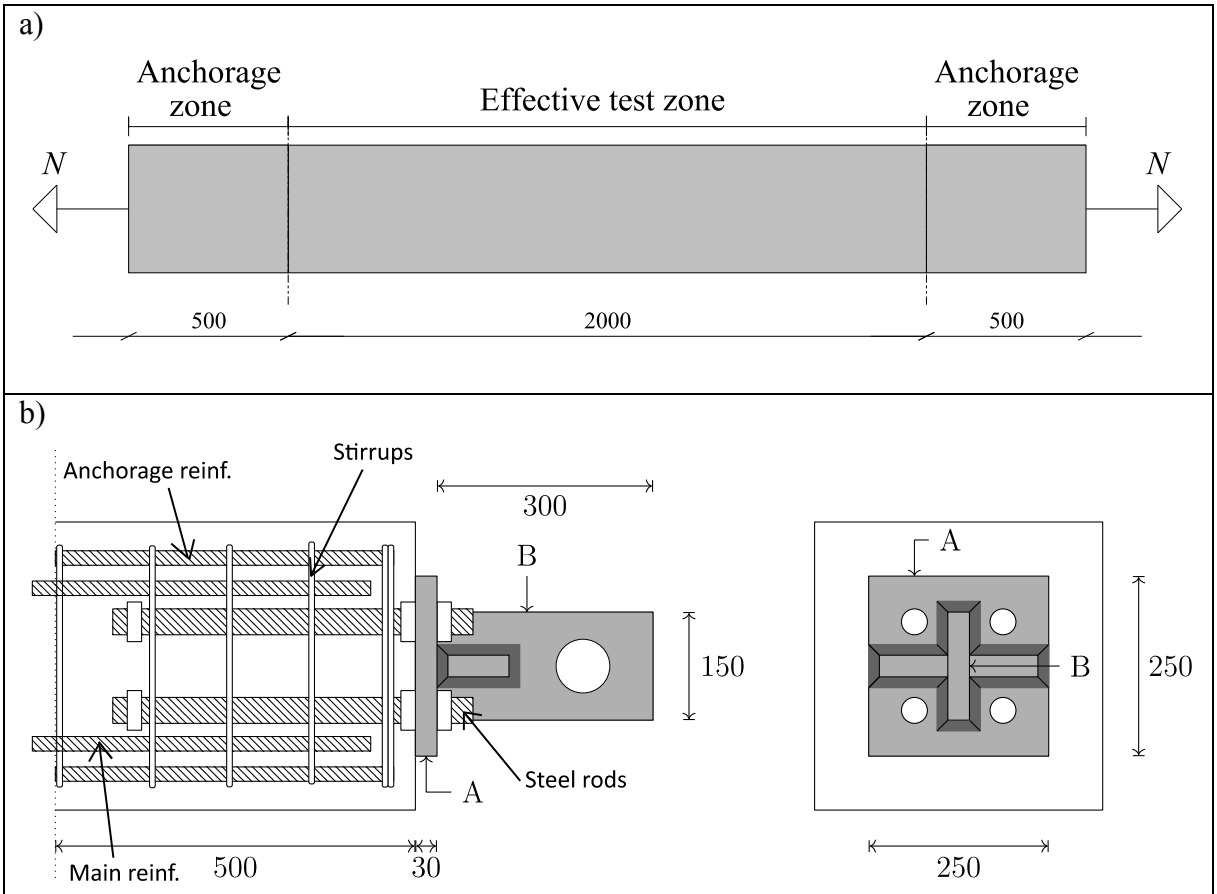

Fig. 5. Test set-up: a) Test set-up for RC ties; b) Anchorage zone details

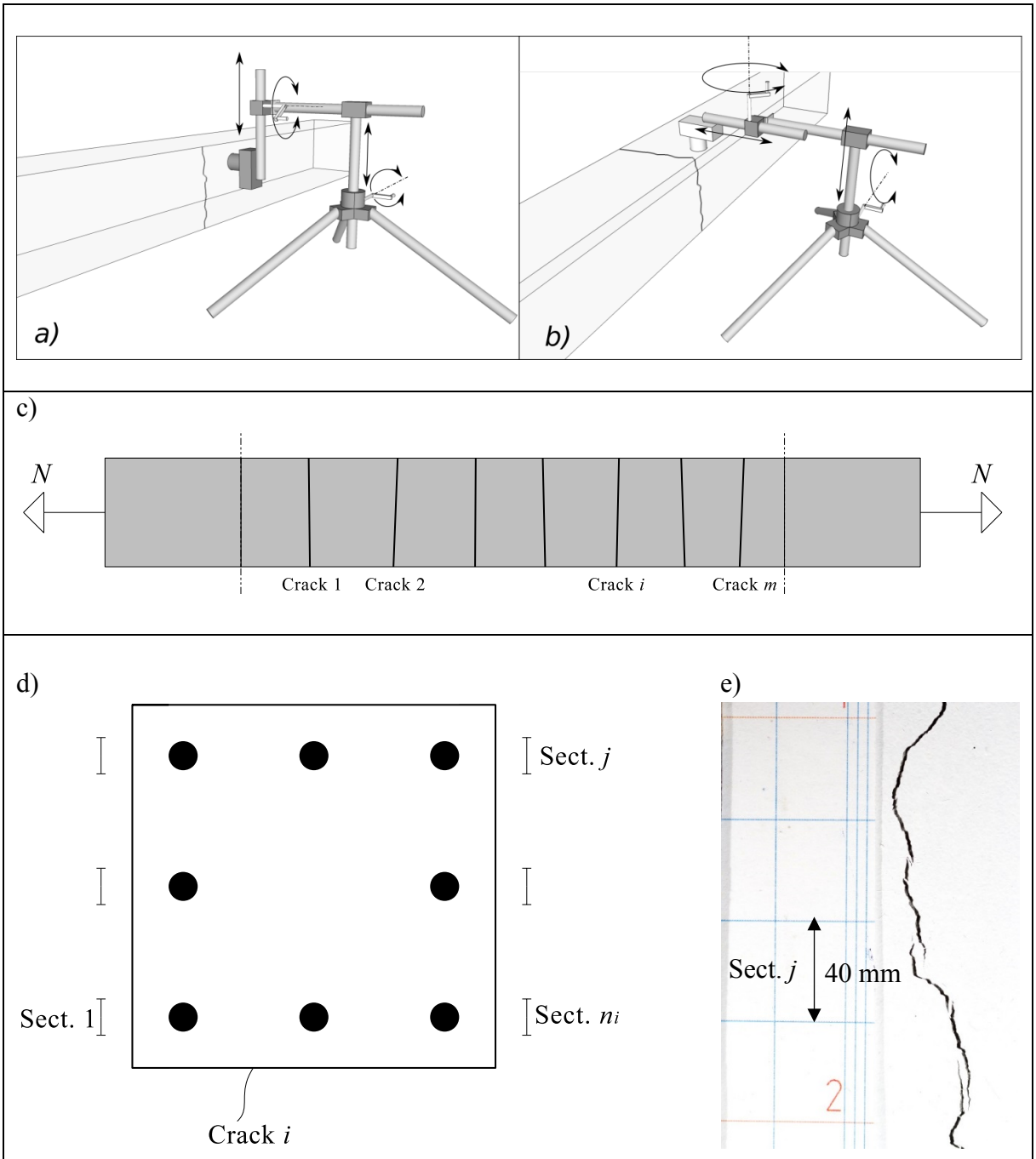

Fig. 6. Measuring crack widths: a) Set-up for measuring crack widths with DSLR camera section-wise at vertical faces; b) Set-up for measuring crack widths with DSLR camera section-wise at top faces; c) Numbering of the cracks formed; d) n_i measured section crack widths at the level of the reinforcement for the formed crack *i*; e) Cracks were averaged over a length of 40 mm at section *j* due to the inhomogeneous propagation of cracks.

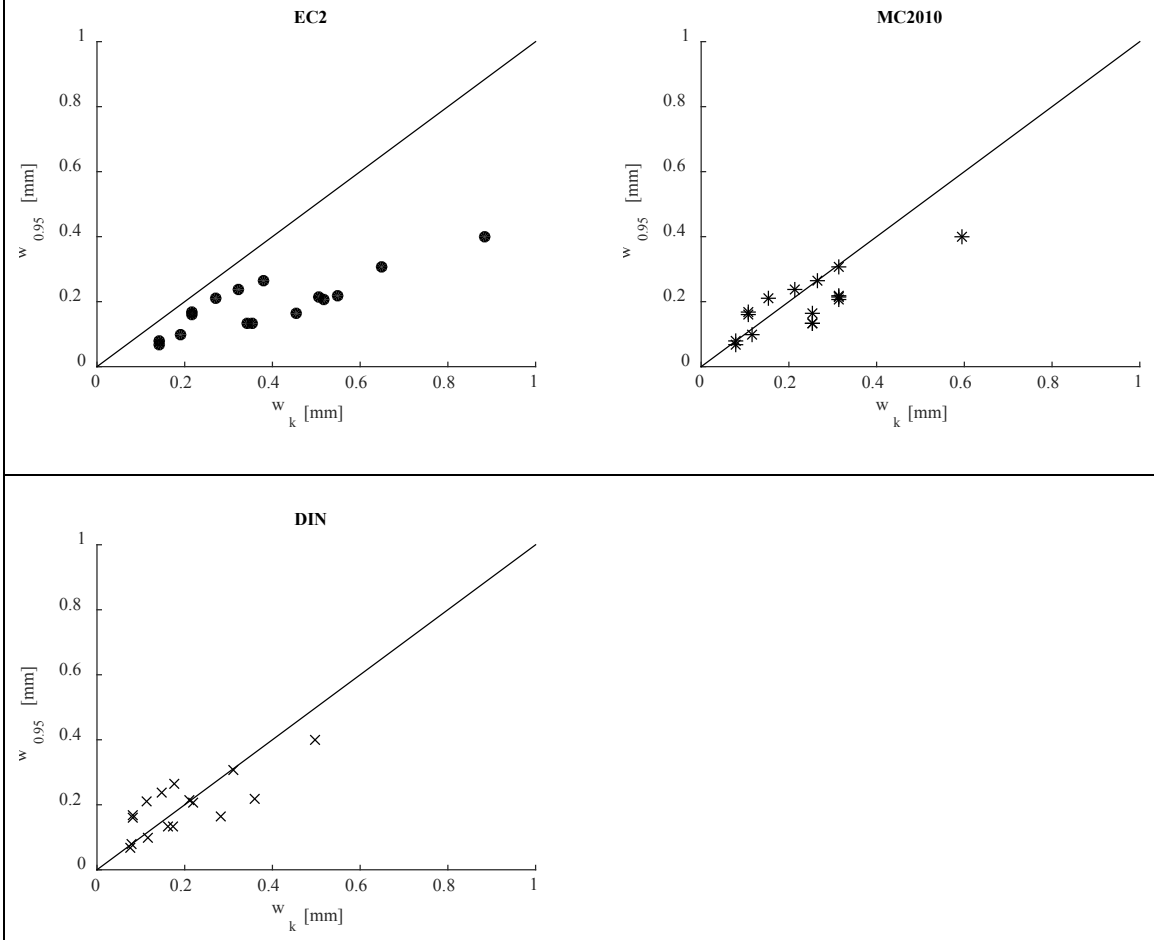

Fig. 7. The modelling uncertainty for EC2, MC2010 and DIN

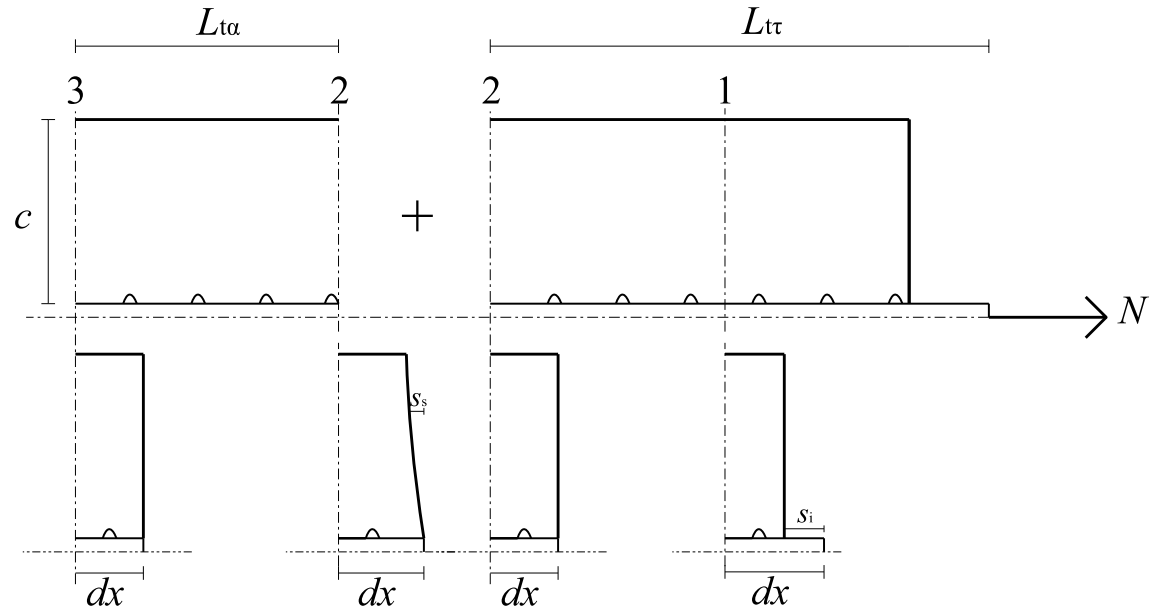

Fig. 8. Composed transfer length formulas conceptually visualized

Table 1. Material properties of concrete at 28 days.

Specimen	Date of test	Measured f_c [MPa]	Mean f_c [MPa]	Measured f_{ct} [MPa]	Mean f_{ct} [MPa]	Measured E_c [GPa]	Mean E_c [GPa]
1	March 03, 2017	74.1		3.98		27.3	
2	March 03, 2017	73.2	74.3	4.03	4.14	27.2	27.4
3	March 03, 2017	75.5		4.41		27.6	

Table 2. Statistical properties showing the number of total measured crack widths n_{tot}, the mean $\bar{y}_{\mathrm{tot}}$ and the variance s_{tot} in a member. $s^2_{\mathrm{tot,w}}/s^2_{\mathrm{tot}}$ indicates the contribution of the within-cracks variation to the total variance, while $w_{0.50}$ and $w_{0.95}$ respectively shows the median and 95%-fractile. These values are obtained by assuming that the crack widths are log-normally distributed.

Member	P [kN]	σ_s [MPa]	n_{tot}	$\bar{y}_{\mathrm{tot}}$	s_{tot}	$s^2_{\mathrm{tot,w}}/s^2_{\mathrm{tot}}$	$w_{0.50}$ [mm]	$w_{0.95}$ [mm]
F-20-40	503	200	42	-2.53	0.31	0.77	0.08	0.13
S-20-40	520	207	6	-2.27	0.11	1.00	0.10	0.13
	667	265	6	-2.07	0.12	1.00	0.13	0.16
	808	321	68	-2.05	0.32	0.61	0.13	0.22
F-32-40	753	117	51	-2.90	0.22	0.71	0.06	0.08
S-32-40	743	115	30	-3.15	0.27	0.65	0.04	0.07
	1012	157	50	-2.91	0.34	0.84	0.05	0.10
F-20-90	585	233	30	-1.93	0.21	0.74	0.15	0.21
S-20-90	574	228	42	-1.99	0.26	0.60	0.14	0.21
	736	293	42	-1.64	0.27	0.50	0.19	0.31
	1003	399	54	-1.44	0.31	0.36	0.24	0.40
F-32-90	804	125	41	-2.47	0.37	0.68	0.08	0.16
S-32-90	805	125	36	-2.36	0.34	0.44	0.09	0.17
	1004	156	47	-2.27	0.42	0.27	0.10	0.21
	1201	187	47	-2.11	0.40	0.31	0.12	0.24
	1363	212	45	-1.91	0.34	0.35	0.15	0.27

Table 3. Load steps and the corresponding crack widths and cracking stages in each member.

	Load		Crack width				Cracking stage			
Member	P [kN]	σ_s [MPa]	$w_{k,EC2}$	$w_{k,MC2010}$	$w_{k,DIN}$	$w_{0,95}$	EC2	MC2010	DIN	Observed
F-φ20-c40	503	200	0.34	0.25	0.16	0.13	F	F	F	F
S-φ20-c40	520	207	0.35	0.25	0.17	0.13	F	F	F	F
	667	265	0.45	0.25	0.28	0.16	F	F	F	S
	808	321	0.55	0.31	0.36	0.22	F	S	S	S
F-φ32-c40	753	117	0.14	0.08	0.08	0.08	F	F	F	F
S-φ32-c40	743	115	0.14	0.08	0.08	0.07	F	F	F	S
	1012	157	0.19	0.12	0.11	0.10	F	S	S	S
F-φ20-c90	585	233	0.52	0.31	0.22	0.21	F	F	F	F
S-φ20-c90	574	228	0.51	0.31	0.21	0.21	F	F	F	F
	736	293	0.65	0.31	0.31	0.31	F	F	F	S
	1003	399	0.88	0.59	0.50	0.40	F	S	S	S
F-φ32-c90	804	125	0.22	0.11	0.08	0.16	F	F	F	F
S-φ32-c90	805	125	0.22	0.11	0.08	0.17	F	F	F	F
	1004	156	0.27	0.15	0.11	0.21	F	S	S	S
	1201	187	0.32	0.21	0.15	0.24	F	S	S	S
	1363	212	0.38	0.26	0.18	0.27	S	S	S	S

Table 4. Statistical properties for the modelling uncertainty showing mean μ_θ, standard deviation σ_θ, coefficient of variation V_θ, minimum and maximum observed values and the number of observations where $\theta > 1$.

	μ_θ	σ_θ	V_θ	Min	Max	$n(\theta > 1)$
EC2	0.54	0.17	0.32	0.36	0.78	0
MC2010	0.93	0.38	0.40	0.52	1.58	5
DIN	1.17	0.55	0.47	0.58	2.03	7

Table 5. Crack distances. $L_{t\alpha}$ and $L_{t\tau}$ respectively indicates the contribution from the no-slip and the slip theory to the maximum transfer length $L_{t,max}$, where the calculated maximum crack distance is given as $S_{r,max} = 2L_{t,max}$. The measured values from the experiments for the maximum crack distance and the mean crack distance $S_{r,m}$ are also shown.

	Load		EC2 [mm]			MC2010 [mm]			DIN [mm]	Measured values [mm]	
Member	P [kN]	σ_s [MPa]	$2L_{t\alpha}$	$2L_{t\tau}$	$S_{r,max}$	$2L_{t\alpha}$	$2L_{t\tau}$	$S_{r,max}$	$S_{r,max}$	$S_{r,max}$	$S_{r,m}$
S-20-40	808	321	136	433	569	80	354	434	353	250	163
S-32-40	1012	157	136	271	407	80	221	301	221	240	178
S-20-90	1003	399	306	433	739	180	354	534	353	290	217
S-32-90	1363	212	306	271	577	180	221	401	221	320	266